Underwater radiated noise from modern commercial ships

Megan F. McKenna[a)]

Scripps Institution of Oceanography, University of California, San Diego, 9500 Gilman Drive, La Jolla, California 92093-0205

Donald Ross

2404 Loring Street, Box 101, San Diego, California 92109

Sean M. Wiggins and John A. Hildebrand

Scripps Institution of Oceanography, University of California, San Diego, 9500 Gilman Drive, La Jolla, California 92093-0205

Underwater radiated noise measurements for seven types of modern commercial ships during normal operating conditions are presented. Calibrated acoustic data (<1000 Hz) from an autonomous seafloor-mounted acoustic recorder were combined with ship passage information from the Automatic Identification System. This approach allowed for detailed measurements (i.e., source level, sound exposure level, and transmission range) on ships of opportunity. A key result was different acoustic levels and spectral shapes observed from different ship-types. A 54 kGT container ship had the highest broadband source level at 188 dB re 1μPa@1m; a 26 kGT chemical tanker had the lowest at 177 dB re 1μPa@1m. Bulk carriers had higher source levels near 100 Hz, while container ship and tanker noise was predominantly below 40 Hz. Simple models to predict source levels of modern merchant ships as a group from particular ship characteristics (e.g., length, gross tonnage, and speed) were not possible given individual ship-type differences. Furthermore, ship noise was observed to radiate asymmetrically. Stern aspect noise levels are 5 to 10 dB higher than bow aspect noise levels. Collectively, these results emphasize the importance of including modern ship-types in quantifying shipping noise for predictive models of global, regional, and local marine environments. © *2012 Acoustical Society of America*. [DOI: 10.1121/1.3664100]

I. INTRODUCTION

The underwater acoustic output generated by commercial ships contributes significantly to ambient noise in the ocean (e.g., Wenz, 1962; Ross, 1976; Wagstaff, 1981; Hildebrand, 2009). Underwater noise from commercial ships is generated during normal operation, most notably from propeller cavitation which is known to peak at 50–150 Hz but can extend up to 10 000 Hz (Ross, 1976).

The history of commercial shipping is defined not only by increases in the number of ships to support burgeoning global trade, but also increases in ship size, propulsion power, and sophistication. The total gross tonnage (GT) of ships quadrupled between 1965 and 2003, at the same time the number of commercial ships approximately doubled, which included new ship designs (Ross, 1993; National Research Council (NRC), 2003; Hildebrand, 2009). This expansion of shipping and ships over the past 4 decades correlated with an increase in deep-ocean noise levels (Andrew *et al.,* 2002; McDonald *et al.,* 2006). Studies of ambient noise on the continental shelf showed relationships with the density of local ship traffic, bathymetry, and sound propagation characteristics; however noise levels can vary significantly depending on the amount of local ship traffic (Hodgkiss, 1990;

Hatch *et al.,* 2008; McDonald *et al.,* 2008; Hildebrand, 2009; McKenna *et al.,* 2009).

Broadband acoustic measurements of radiated noise from individual modern ships under normal operating conditions are needed to advance our understanding of the contribution of shipping noise to the marine environment. Surveys of underwater noise from ships in the last few decades provided information about noise from individual ships operating under various conditions; however, these controlled measurements were made on a limited number of ships and most measurements were from older ships and narrower frequency bands (Ross, 1976; Arveson and Vendittis, 2000; Heitmeyer *et al.,* 2003; Trevorrow *et al.,* 2008). Furthermore, different ship-types were combined into the same analysis, making it difficult to examine dissimilarities in source levels and spectral characteristics (Heitmeyer *et al.,* 2003).

In this study, we took an opportunistic approach to measuring radiated noise from commercial ships transiting the Santa Barbara Channel (SBC), a region off the coast of southern California (Fig. 1). Ships use these lanes when traveling to and from the combined ports of Los Angeles and Long Beach. Acoustic measurements near the seafloor were collected using an autonomous long-term passive acoustic recorder and were combined with ship passage information from the Automatic Identification System (AIS).

Metrics of ship noise, including spatial radiation patterns, source levels, spectral characteristics, and sound

---

[a)]Author to whom correspondence should be addressed. Electronic mail: megan.mckenna@gmail.com

exposure levels, are presented for seven merchant ship-types: container ships, vehicle carriers, bulk carriers, open hatch cargo ships, and chemical, crude oil and product tankers. Most ships were built after 1990. Bahtiarian (2009) provided a standard for measuring underwater noise generated by ships which provided specific guidelines for measurement set up, instrumentation and data processing. We incorporated some of the specifications when feasible, but acknowledge our experimental design has some limitations. The strength of our study is the measurement of many ships of various types under normal operation.

II. BACKGROUND: MERCHANT SHIP TYPES

The world merchant fleet of modern ships over 100 GT is composed of approximately 100 000 ships, totaling 830 million GT with an average age of 22 years (United Nations Conference on Trade and Development (UNCTD), 2008). The global fleet is composed of a variety of vessel types, categorized based on goods carried. The cargo transported greatly influences designs and operating conditions of different ship-types (Eyres, 2007). This study examines a variety of these ship-types to understand differences in acoustic signatures.

Ships designed to carry bulk goods include both bulk carrier and tanker ship-types (35% of global fleet). The cargo is transported in holds below the water level (Eyres, 2007). Tankers are categorized as crude oil tankers, product, or chemical tankers (UNCTD, 2008). Crude oil tankers, generally the largest, transport unrefined crude oil from the location of extraction to refineries. Product tankers carry refined petrochemicals. Chemical tankers are similar in size to product tankers, but carry chemical products. General cargos occupy the largest single category (32%) in the world merchant fleet (UNCTD, 2008). Open hatch cargo ships are one of the many groups of general cargos, which transport any unitized cargo (i.e., pallets) in cargo holds.

Container ships, designed to carry cargo pre-packed into containers, did not exist prior to the 1960s: since 1990 container trade has increased by a factor of 5. Currently, these ships make up 13% of the world's fleet in terms of deadweight tonnage, and are predicted to increase (UNCTD, 2010). Container ships carry cargo in rectangular containers units within the fuller portion of the hull, arranged in tiers stacked on the deck of the ship (Eyres, 2007). Vehicle carriers, a specialized group of container ships, transport automobiles in compartments. These ships have a high box-like form above the waterline to accommodate as many vehicles as possible.

III. METHODS

A. Acoustic recordings

In April 2009, a high frequency acoustic recording package (HARP) was deployed in the SBC (34°16.2′N and 120°1.8′W) at a depth of 580 m (Fig. 1). HARPs are bottom-mounted instruments containing a hydrophone, data logger, low drift rate clock, battery power supply, ballast weights, acoustic release system, and flotation (Wiggins and Hildebrand, 2007). The hydrophone sensor is tethered to the instrument and buoyed approximately 10 m above the seafloor. The hydrophone sensor includes two transducers, resulting in a sampling frequency of 200 kHz. Acoustic data used in this study were decimated to a sampling frequency of 2 kHz. All acoustic data were corrected based on hydrophone sensitivity calibrations performed at Scripps Whale Acoustics Laboratory and at the U.S. Navy's Transducer Evaluation Center facility in San Diego, California.

All acoustic measurements were taken along the starboard side of ships transiting in the northbound shipping lane of the SBC (Fig. 1). The closest point of approach (CPA) of a ship to the HARP was measured as the slant
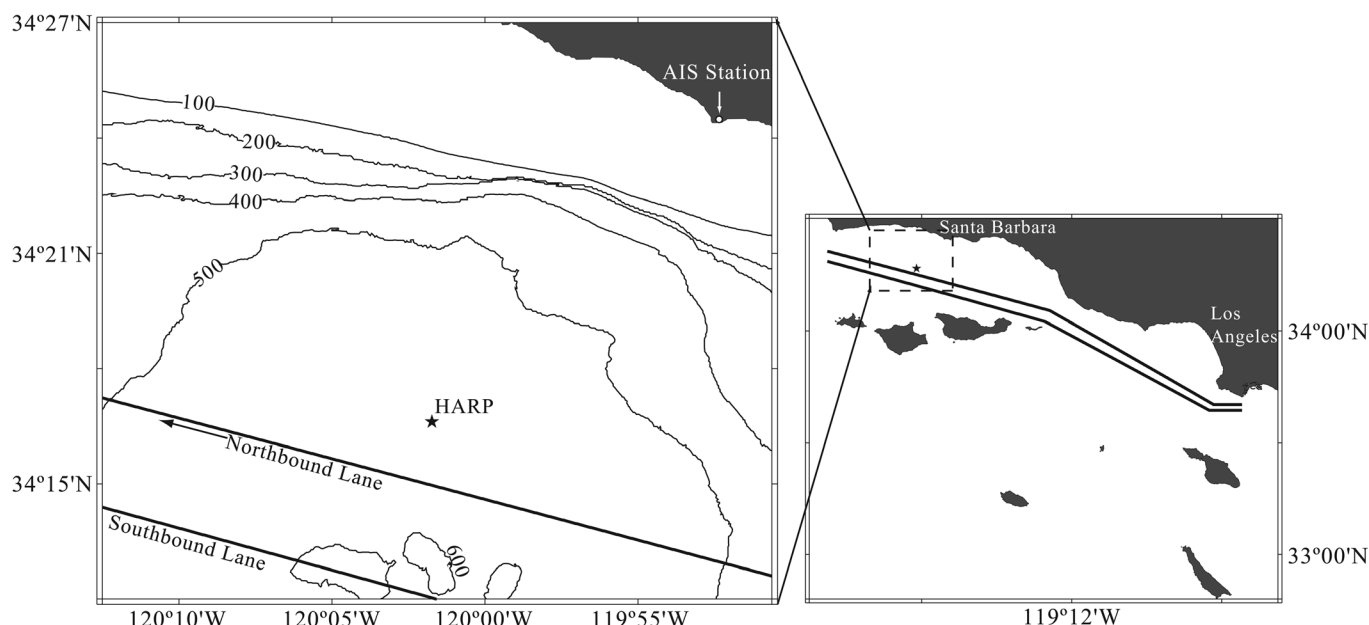

FIG. 1. Map of the Santa Barbara Channel. The northbound and southbound shipping lanes and 100 m bottom contours are shown. (HARP = black star, AIS station = white dot).

range to the HARP, based on the depth of the HARP hydrophone (570 m) and the surface distance of the ship to the HARP. Ship positions were determined from the AIS (see next section for description). Only northbound ships were analyzed to minimize the ranges from the ships to the HARP; at CPA northbound ships are approximately 3 km from the HARP compared to southbound ships that are 8 km at CPA. Bow aspect ship noise measurements occurred as the ships approached CPA; stern aspect measurements were taken after CPA.

The acoustic data corresponding to CPA derived from ship passage information (i.e., AIS data) were manually verified and evaluated for the presence of a single ship. Ship passages were eliminated from the analysis if the passage of another ship occurred within 1.5 h of CPA or if vocalizing marine animals (e.g., whales, fish) were present. To provide broad comparisons between different ship-types, this study includes a small sub-set of examples from a larger database of ship passages.

B. Ship passage information

Commercial vessel activity was monitored in the SBC using AIS (Tetreault, 2005) located on the campus of the University of California at Santa Barbara (UCSB) (34°24.5′N and 119°52.7′W) (Fig. 1). AIS signals from vessels in the region were received using a very high frequency (VHF) omni-directional antenna and a radio (Icom IC-PCR1500 receiver) connected to a computer. The software program *Ship-Plotter* (ver. 12.4.6.5, COAA) was used to decode the VHF signal and archive daily logs. All archived AIS data were downloaded and imported into a *PostgreSQL* database. Queries were designed to extract information on northbound ships passing the HARP during the recording period. The information extracted from the AIS database for each ship included a time stamp, speed, heading, latitude and longitude, unique ship identification, ship name, general ship-type, total length, and maximum draft.

Atmospheric conditions, shadow zones, and variability in ship AIS transmissions introduce irregularity in AIS points received. To standardize each ship track, the AIS point transmissions, including ship heading and speed, were interpolated to create a track with a position every 10 s. The surface current speed and direction during the passage of each ship were obtained from archived data at the UCSB surface current mapping project (Institute for Computational Earth System Sciences (ICESS), 2009). The speeds over ground from the AIS data were adjusted to actual speed through the water by removing the effect of surface current speed and direction. Additional information for each ship (i.e., ship-type, gross tonnage, engine specifics, and horse power) was extracted from the World Encyclopedia of Ships from Lloyd's Registry of Ships.

C. Spectral characteristics of 1-h ship passages

Estimates of background noise in three frequency bands (i.e., 40, 95, and 800 Hz) were compared to received sound levels (RLs) during 1-h ship passages. Background noise levels in the SBC were previously measured when ships

were not present, providing a noise baseline for the region (McKenna *et al.*, 2009). Background noise levels were measured with the HARP at the same site as this study were reported to be 80 dB re 1 μPa^2/Hz at 40 Hz, 68 dB re 1 μPa^2/Hz at 95 Hz, and 63 dB re 1 μPa^2/Hz at 800 Hz (see Fig. 2 of McKenna *et al.*, 2009).

One-hour ship passages were divided into 60 one-minute bins, for 30 min prior to CPA and 30 min after CPA. For each 1-min interval during the ship passage, RLs were measured. For each 1-min interval, the time series was processed using a fast-Fourier transform and a Hanning window with an FFT length of 2000 samples and no overlap. The fast-Fourier transforms resulted in mean pressure squared values in 1-Hz bins for 20–1000 Hz. The data were then converted to sound spectrum levels expressed as decibels references to a unit pressure density.

The start time of each acoustic measurement was determined from the interpolated ship track, described above. The differences between ship passage RLs and background noise levels for the three frequency bands were reported as a function of time to the ship CPA. The corresponding distance from the ship to the HARP at each 1-min interval was calculated to determine the spatial extent at which noise levels were above background. The range at a given one-minute interval (R_i) was calculated as

$$R_i = \sqrt{(d_{\text{cpa}})^2 + (d_i)^2},\qquad(1)$$

where, d_{cpa} is distance of the ship to the HARP at CPA, d_i is the distance traveled from ship to CPA for a specific 1-min interval. The distance the ship traveled in the 1-min interval d_i was calculated from the speed reported by AIS, corrected for water current speed, and the heading of the ship.

D. Transmission loss

The inverse square law method of sound transmission loss (TL) was used to estimate ship source levels, given the known distance of the ship to the receiver. To validate this approach a TL model using a range dependent parabolic equation (PE) was created, using the Acoustic Toolbox User Interface and Post Processor (Duncan and Maggi, 2005). The model required seabed (i.e., bathymetry and sediment) and water column (i.e., salinity and temperature) properties. Core samples from the seafloor near the HARP site showed sediments of silty layers (Emery, 1960; Hulsemann and Emery, 1961). The sediment characteristics used in the propagation models were based on literature descriptions of the sediment and the geo-acoustic properties associated with that sediment type (Hampton, 1973). We also included a bottom roughness in the models to dampen reflections.

A water column sound speed profile was generated from temperature, salinity and pressure measurements (Mackenzie, 1981) taken at a location close to the HARP (34°15.0′N and 119°54.4′W). The measurements were collected on April 21, 2009, the same month and year the ships in this study transited the region. Water column data were collected as part of the monthly sampling for Plumes and Blooms Program at the Institute for Computation Earth System Science

at the UCSB. Water column data were collected only from the sea surface down to 200 m. Previous studies in this region showed a constant sound speed profile at depths below 200 (Linder and Gawarkiewicz, 2006).

The sound source in the PE model was placed at 7 and 14 m below the sea surface, typical depths of ship propellers. Source frequencies ranged from 22–177 Hz. Horizontal ranges extended from 100 to 5000 m and depths ranged from the sea surface to the seafloor (580 m). The model's spatial resolution was 50 m in depth and 50 m in horizontal range. Acoustic transmission loss at the depth of the hydrophone and ranges from the ships to the HARP were reported.

E. Source levels

Received sound levels at CPA were converted into estimated source levels (SLs) at 1 m relative to 1 μPa. The estimated source level for a given ship (SL_s) was calculated as

$$\mathrm{SL}_s = \mathrm{RL}_{\mathrm{cpa}} + \mathrm{TL}_{\mathrm{cpa}}, \tag{2}$$

where, $\mathrm{RL}_{\mathrm{cpa}}$ is the RL at CPA of the given ship, and $\mathrm{TL}_{\mathrm{cpa}}$ is the sound transmission loss over the CPA distance, calculated using inverse square law method. The time window used for the SL estimate equaled the time it took the ship to travel its length, as suggested in Bahtiarian (2009). AIS provided the speed and length of the ship needed for this calculation. For each ship CPA time window, the time series was processed using a fast-Fourier transform, a Hanning window, an FFT length of 2000 samples, and no overlap. The fast-Fourier transforms results in mean pressure squared values in 1-Hz bins for 20–1000 Hz. The range from the ship to the HARP at CPA was calculated from coordinates of the HARP and the ship, as described above.

Source level estimates are presented in 1-octave and 1/3-octave bands, using the standard center frequencies, and in 1-Hz bands. To determine the 1-octave and 1/3-octave band levels, the mean squared pressure values were summed across the frequencies, and converted back to sound pressure levels expressed as decibels referenced to a unit pressure density. For each ship-type category, the mean SL and standard error were calculated for the 1-octave and 1/3-octave frequency bands.

F. Sound exposure levels

Sound exposure levels (SELs) were estimated for all ships at their CPA distance ($\sim$3 km). The SEL for each ship passage was calculated by integrating the square of the received pressure waveform over the duration of the passage. The duration of the passage was determined from a cumulative sum of RLs for a 30 min period after CPA. We defined the integration time cutoff for the duration of the ship passage when the difference in RL cumulative summation was less than 0.1 dB. The duration of the passage, or integration time, is dependent on the distance from the ship to the receiver and the speed of the ship.

An equation for calculating SEL at various ranges from the sound source (i.e., ship) was established. Ranges of interest (ROI) ranged from 500 m to 15 km and were estimated based on how far the ship travel in each 1-min interval using the speed of the ship. This step was necessary because AIS does not provide regular positional updates. The first step was to calculate the RLs at each ROI from the ship source level (SL) estimates minus TL from the source to the ROIs. Second, the distances from the HARP to ship locations during the 30 min stern passage (at 1-min intervals) were determined based on a ratio of the CPA distance to the ROI distance. RLs during this passage were then calculated and the integration time and SEL were set to when the cumulative sum did not change by more than 0.1 dB. Last, an exponential equation was fit to the SEL, as a function of range, and constants are reported for each ship in this study:

$$\mathrm{SEL} = ar^b, \tag{3}$$

where a and b are constants specific to each ship, and r is the range in meters from the source.

IV. RESULTS

A total of 29 ships that transited the northbound shipping lane in the SBC in April 2009 were analyzed. The ships were divided into seven ship-type categories as designated by the World Shipping Encyclopedia from Lloyd's Registry of Ships. Table I summarizes the design and operational conditions as well as the measured received and estimated broadband source levels for each transiting ship. Within each of the seven ship-type categories, the vessels had similar sizes and traveled at similar speeds.

A. Spectral characteristics of 1 h ship passages

One-hour spectrograms of a container ship, bulk carrier and product tanker RLs (illustrated in Fig. 2, selected ships are designated as "a" in Table I) revealed distinct differences in radiated noise related to ship-type. Two dominant features shown are tonal lines below 100 Hz and the "U" shaped pattern centered at CPA (Fig. 2). Tonal lines result from propeller blade cavitation and their harmonics (Ross, 1976). The U-shaped interference patterns at the higher frequencies (>100 Hz) are caused by constructive and destructive interference from a dipole sound source; or in other words, the interactions of the direct and surface reflected propagation paths as the point source moves along the source-receiver path (Albers, 1964; Ross, 1976; Wales and Heitmeyer, 2002). This phenomenon is known as Lloyd's Mirror Effect and is dependent on the depth of the source and receiver, distance of the source to the receiver, water column properties, and bottom reflection (Wilmut et al., 2007).

Another pattern seen in the spectrogram plots of Fig. 2 is the asymmetry between the bow and stern aspects in the lower frequencies, with more radiated energy at the stern aspects (i.e., positive time from CPA). The temporal and spatial extents were different depending on the ship-type. As the container ship approached CPA, the RLs at 40 Hz rose above background at 16 km from the receiver [Fig. 2(a), bottom panel]. As the container ship traveled away from the receiver, noise levels at 40 Hz stayed above background for over 30 min (i.e., >20 km distance from the receiver). At 95 and 800 Hz, container ship RLs were above

96

J. Acoust. Soc. Am., Vol. 131, No. 1, January 2012

McKenna et al.: Underwater ship noise

TABLE I. Summary of commercial ship characteristics.

| Ship type | Ship information (Lloyd's Registry of ships) | | | | | Acoustic measurements | | | | Sound exposure level at 3 km[c] | | | |
	MMSI number	Ship length (m)	Year built	Gross tonnage (10^3)	Horse power (10^3)	Ship speed (ms^{-1})	Range at CPA (km)	Received level at CPA[b]	Source level at 1 m[b]	dB	minutes	$a(r)$[b] a	b
Container Ships	636090869	294	2005	54.6	62.2	10.6	3.1	114.9	184.7	123.1	12	217.4	−0.071
	352919000	294	1994	53.1	42.1	10.7	2.6	116.1	184.5	122.3	11	216.8	−0.072
	235007500	294	2004	53.5	55.9	10.7	3.0	117.0	186.6	124.9	12	218.8	−0.070
	353287000	294	2003	53.8	67.2	10.9	3.2	114.9	185.0	123.4	12	217.6	−0.071
	548719000[a]	294	1993	53.4	42.1	11.0	3.0	114.6	184.2	122.5	12	216.9	−0.072
	211207740	298	1993	53.8	49.6	11.2	2.9	118.9	188.1	126.1	12	219.7	−0.070
Vehicles Carriers	413075000	173	1984	33.1	10.7	7.8	2.9	110.6	180.0	119.3	14	214.5	−0.074
	353788000	180	1989	47.6	14.7	8.5	3.0	108.6	178.1	117.1	14	213.0	−0.075
	232872000	199	2006	61.3	16.5	8.5	3.0	111.3	180.8	119.9	14	215.0	−0.073
	636011280	175	2000	37.9	12.2	9.1	3.3	111.8	182.2	121.4	14	216.1	−0.072
Bulk Carriers	576915000	189	2004	29.7	9.3	7.1	3.4	115.2	185.8	125.9	16	219.5	−0.070
	371978000	229	2006	42.9	13.3	7.1	3.2	114.9	185.1	125.0	16	218.9	−0.070
	240537000	225	2005	40.0	12.7	7.3	3.1	116.0	185.9	125.7	15	219.3	−0.070
	371940000	190	2007	30.7	11.0	7.3	2.7	115.6	184.2	123.4	14	217.6	−0.071
	440223000[a]	167	1997	16.3	9.1	7.4	3.0	117.9	187.4	127.0	15	220.4	−0.069
Open Hatch Cargo Ships	477657600	199	2007	29.8	12.9	6.7	3.4	111.2	181.8	122.1	16	216.6	−0.072
	257313000	197	1986	27.2	10.1	6.7	3.1	109.0	178.8	118.8	16	214.2	−0.074
	477653500	190	2007	20.2	9.0	7.3	2.8	114.8	183.8	123.2	14	217.4	−0.071
	563496000	213	1995	37.2	14.1	7.3	3.0	111.5	181.1	120.7	15	215.6	−0.073
Chemical Products Tankers	355799000	148	1985	10.8	6.9	4.6	3.4	114.9	184.9	124.3	14	218.3	−0.071
	636010515	181	1996	26.2	11.3	6.2	3.3	106.0	176.6	118.0	19	213.6	−0.074
	235007540	182	2004	30.0	12.9	7.1	3.4	111.9	182.4	123.0	17	217.3	−0.071
	352329000	149	1993	10.8	8.2	8.0	3.2	112.5	183.1	123.2	16	217.4	−0.071
Crude Oil Tankers	564924000	241	2003	56.4	16.0	6.5	3.5	108.7	179.4	119.9	17	215.0	−0.073
	636012853	243	2006	57.2	18.4	6.6	3.1	112.1	182.1	122.2	16	216.7	−0.072
	636090885	229	2000	37.0	13.0	7.5	2.9	112.1	181.3	120.7	14	215.6	−0.073
Product Tankers	371604000	182	2005	28.1	12.6	7.1	2.9	109.3	178.5	118.0	15	213.6	−0.074
	319768000[a]	228	2007	42.4	18.4	7.5	3.1	112.7	182.7	122.4	15	216.8	−0.072
	371924000	180	2006	28.8	12.9	8.0	3.4	111.2	181.8	121.5	15	216.2	−0.072

[a]Ships shown in Fig. 2.
[b]dB re 1 μPa^2 (20–1000 Hz).
[c]dB re 1 μPa^2 (20–1000 Hz) × seconds; r = range in meters.
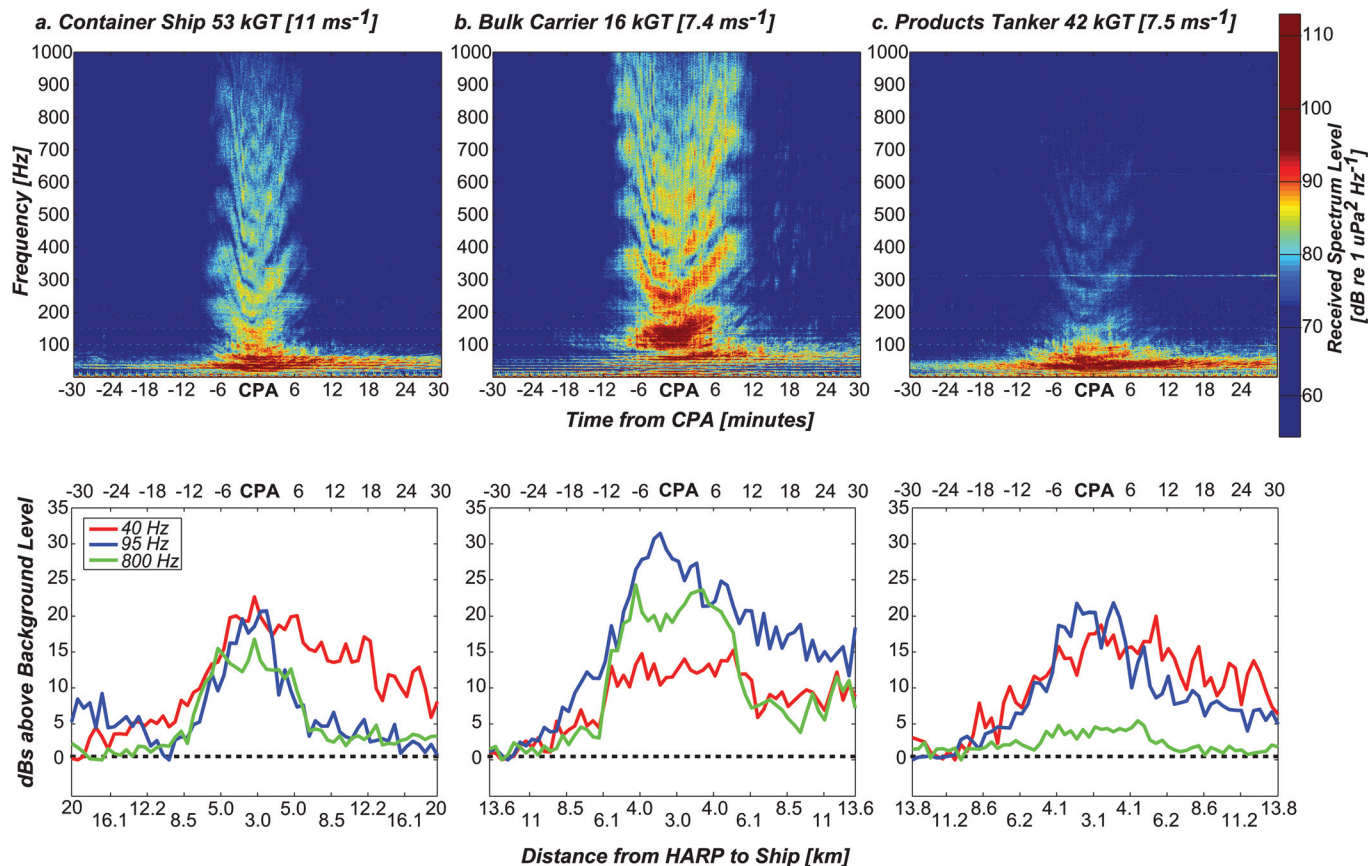
FIG. 2. Received sound levels during 1-h passages of three different ship-types: (a) Container ship (MMSI 548719000). (b) Bulk carrier (MMSI 440223000). (c) Product tanker (MMSI 319768000). Figures are centered at CPA of the ship to the HARP. Negative CPA is bow aspect; whereas positive values are stern aspect. Top figure series shows the received levels as color (dB re 1 μPa^2/Hz) during a 1-h window around the passage of the ships, using sequential 5 s spectral averages to form the long-term spectrogram (Hanning window, FFT length of 2000 samples and 80% overlap). Bottom figure series show measured RL above an estimate of background noise level. The corresponding distance traveled over that 1-h period is shown on the x axis on the bottom graphs; this scale is dependent on the speed of the ship.

background symmetrically at the bow and stern aspects, approximately 8.5 km [Fig. 2(a), bottom panel]. As the bulk carrier approached CPA, noise levels in the 95 Hz band were elevated above background first, at a distance of 11 km from the receiver [Fig. 2(b), bottom panel]. At the stern aspect, noise levels in all bands remained above background for the entire 30 min period (>13 km), with the 95 Hz band having the highest levels. Low-frequency noise levels (<100 Hz) for the product tanker were above background for almost the entire 1-h passage of the ship, with more acoustic energy at the stern aspect. The spatial extent at the bow of the tanker was 11 km, whereas the stern aspect was >13 km.

The frequency content of the radiated noise varied by ship-type. The RLs from the container ship were highest at frequencies below 100 Hz [Fig. 2(a)]; although higher frequency noise also was produced during the passage. RLs were highest at CPA with measured levels about 20 dB above background at 95 and 40 Hz, and about 15 dB above background at 800 Hz [Fig. 2(a), bottom panel]. The RLs from the bulk carrier were highest at frequencies near 100 Hz [Fig. 2(b)]. At CPA, the noise levels were about 30 dB above background at 95 Hz and around 20 dB above at 800 Hz, but only 10 dB above background at 40 Hz. Unlike the bulk carrier, most of the acoustic energy from the product tanker was

below 100 Hz [Fig. 2(c)]. The levels at 800 Hz rose above background by <5 dB, resulting in the lowest RLs near CPA for high frequency compared to the other two ship-types.

The broad-band RLs at CPA were highest for the bulk carriers and container ships (Table I, ~116 dB re 1 μPa^2 at 20–1000 Hz). The tankers, open hatch cargos, and vehicle carriers all had similar broadband received levels at CPA (Table I, ~111 dB re 1 μPa^2 at 20–1000 Hz). These values are somewhat comparable; given that the CPA distance from the ships to the HARP only ranged from 2.6 to 3.5 km (Table I). The source levels estimated at 1 m provide a better comparison (see next section).

B. Source levels

The water column properties in April 2009 were dominated by cold up-welled water with a thin (<10 m) warm surface layer present, likely from solar heating [Fig. 3(a)]. The up-welled water is commonly observed throughout the region in the spring (McClatchie *et al.,* 2009). Based on these water column properties and known sediment properties for the basin, propagation model TL curves for the 63 Hz one-octave band and two source depths are shown to be similar to spherical spreading model where $\text{TL} = 20 \log_{10}(\text{range[m]})$
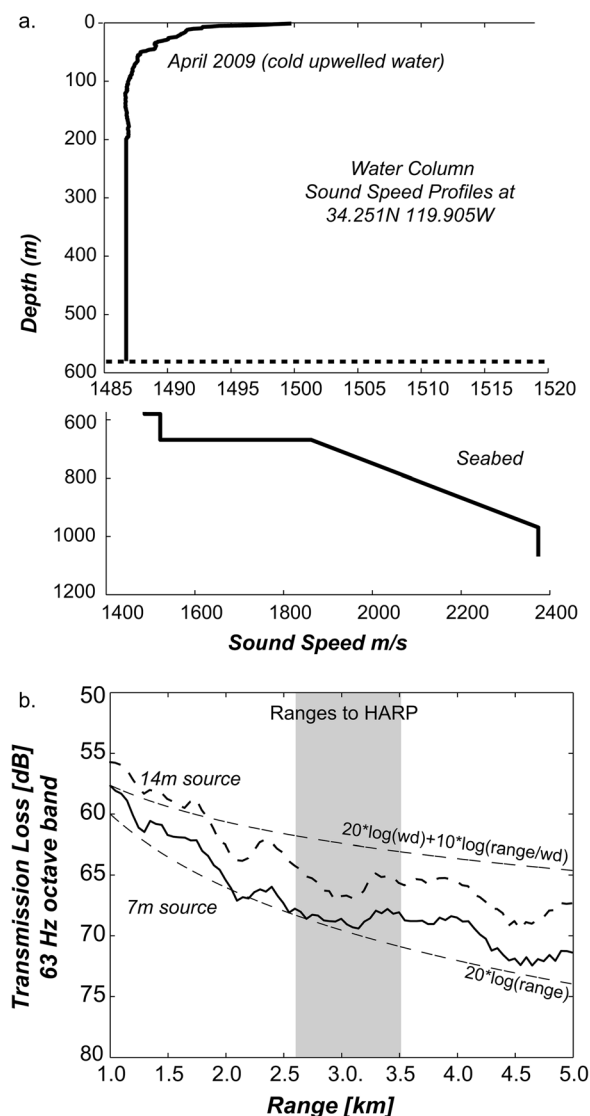
FIG. 3. Region specific PE transmission loss model. (a) Sound speed depth profile for water column and sediment during April 2009. (b) Sound propagation loss for 63 Hz one-octave band at depths of 510–570 m for different source depths (14 and 7 m). The ranges from the ships to the HARP are shaded in gray (wd = water depth at acoustic receiver in m).

[Fig. 3(b)]. The effects of seawater absorption can be ignored at these short ranges and low frequencies (Fisher and Simmons, 1977; Jensen *et al.,* 1993). Propagation loss models for the 1/3-octave frequency bands investigated were found to be similar at ranges comparable to the CPA distance (∼3 km); however, TL variability was found to be related to source depth. Decreasing the source depth from 14 to 7 m increased TL bands by 2–4 dB at the ranges of interest [Fig. 3(b)]. Given the sensitivity of the PE prediction to source depth, variability in sound speed profile, and other possible range dependent environmental effects, the use of inverse power law to calculate SL seems reasonable yet generates a slight overestimate of the true TL [Fig. 3(b)].

A spherical spreading model was used to estimate source levels of each ship at CPA from the received levels at the HARP for the full band 20–1000 Hz (Table I) and for 1-octave, 1/3-octave and 1-Hz bands (Fig. 4). A container ship

traveling at 11.2 ms^{-1} (21.7 knots) had the highest estimated broadband source level (188.1 dB re 1 μPa^2 20–1000 Hz); whereas, a chemical product tanker traveling at 6.2 ms^{-1} (12.1 knots) had the lowest estimated source level (176.6 dB re 1 μPa^2 20–1000 Hz). A different chemical tanker (MMSI 355799000) had surprisingly high SL (184.9 dB re 1 μPa^2 20–1000 Hz) given its size and slow speed. On average, the container ships and bulk carriers had the highest estimated broadband source levels (186 dB re 1 μPa^2 20–1000 Hz), despite major differences in size and speed (Table I and Fig. 5). The container ships traveled on average seven knots faster than the bulk carriers and are on average 20 kGT larger.

One-octave band source levels provided the best measurement for averaging over the interference patterns present in the 1/3-octave and 1-Hz bands, yet still captured differences in spectral characteristics of different ship-types (Fig. 4). For example, the bulk carriers clearly have a different acoustic signature compared to container ships, with a distinct peak at 100 Hz. This spectral difference is not captured in the broadband (20–1000 Hz) source level estimate for bulk carriers and container ships; the broadband levels are similar for these ship-types (Table I, Fig. 5).

From Table I, a comparison is made of different ship-types based on ship speed and estimated broadband source levels (Fig. 5). Empirical models to predict sound spectrum of modern merchant ships as a function of a particular ship characteristic proved difficult, given the differences related to ship-type. For example, bulk carriers and container ships had similar source levels, but traveled at different speeds, and while container ships and vehicle carriers showed evidence for increased source level with larger size and faster speeds (Fig. 5), bulk carriers and tankers did not follow the same relationship. Furthermore, the bulk carriers had higher source levels compared to the open hatch cargos, yet both traveled at speeds of 7 ms^{-1} [Figs. 4(b) and 5].

C. Sound exposure levels

At a distance of 3 km SELs were highest for a bulk carrier traveling at 7.4 ms^{-1} and lowest for a vehicle carrier traveling at 8.5 ms^{-1} (127 and 117 dB re 1 μPa^2 s, respectively). The integration time for exposure level at 3 km varied with ship-type. In general, ships traveling faster (i.e., container ships) had shorter integration time (Table I). The longest integration time for the sound exposure above background levels at 3 km was for a chemical product tanker (19 min), the slowest ship in this study (6.2 ms^{-1}).

The SEL equations from Table I are useful for estimating the total acoustic energy at a given distance from the ship while assuming the receiver remains stationary over the integration time shown. For example, using the equation in Table I the broadband SEL at 1 km for a 54.6 kGT container ship would be 166.2 dB re 1 μPa^2 s; the same ship at a distance of 5 km the SEL would be 148 dB re 1 μPa^2 s.

V. DISCUSSION

This study described and compared acoustic levels and spectral characteristics from a variety of modern ship-types opportunistically under normal operating conditions. The
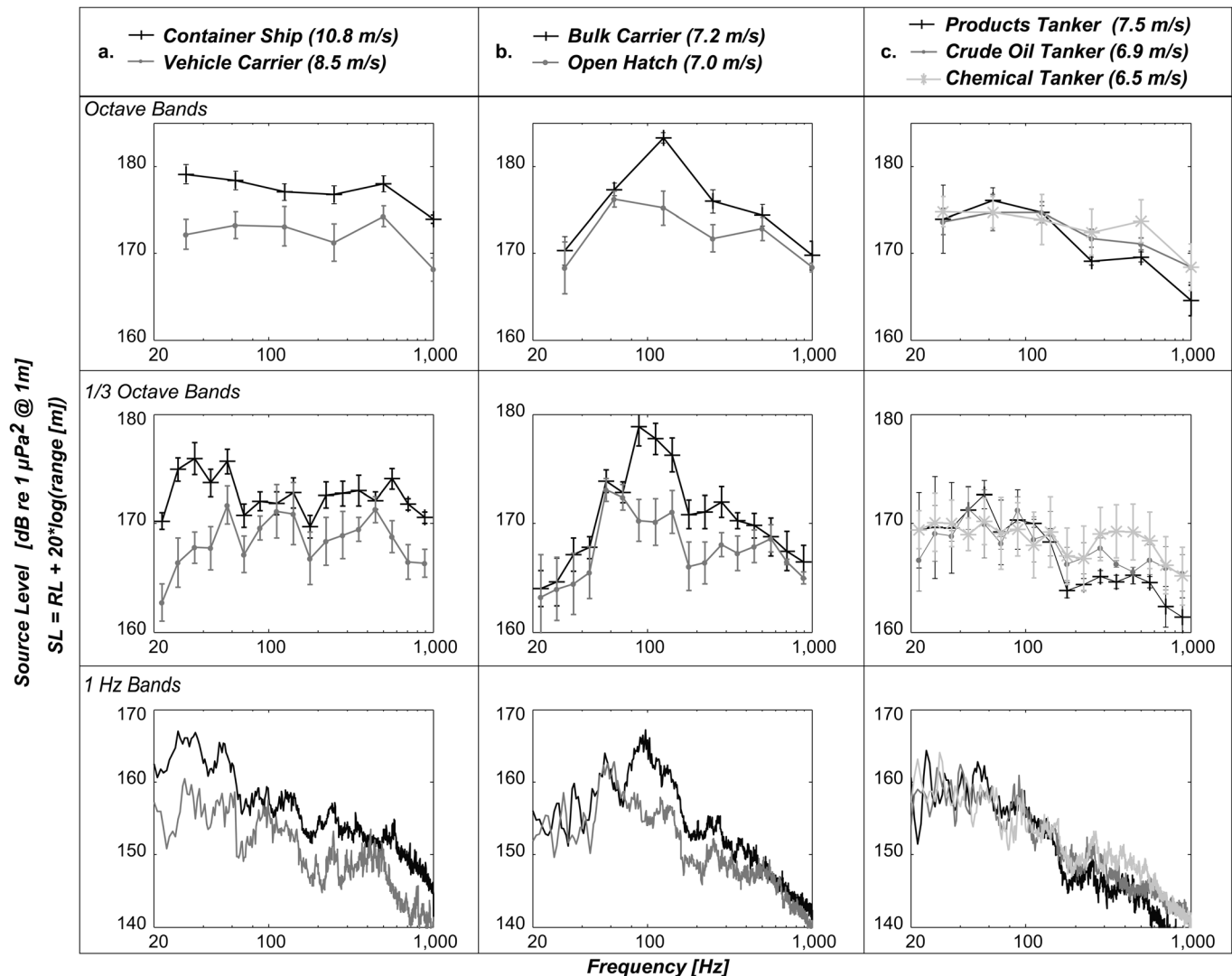
FIG. 4. Ship source levels for (a) container ships and vehicle carriers, (b) bulk carriers and open hatch cargos, and (c) three types of tankers. Top two series of figures show one-octave and 1/3 octave bands, with mean and standard errors. Bottom series shows the 1 Hz band levels.

results showed unique ship-type acoustic signatures important for predicting underwater noise levels and understanding acoustic impacts on marine life. In addition to using long-term, calibrated acoustic measurements, a key component in this analysis was the use of the AIS to provide accurate distances from the transiting ships to the acoustic receiver.

A. Radiated ship noise and ship characteristics

Previous studies of underwater shipping noise provided important details on noise levels from individual ships operating under various conditions. Some of these studies also investigated functional relationships between radiated noise and operating conditions (Ross, 1976; Arveson and Vendittis, 2000; Heitmeyer *et al.,* 2003; Trevorrow *et al.,* 2008). These measurements, however, were made on older ships and in narrower frequency bands. Therefore, making direct comparisons with previous studies is not appropriate given that ships reported in this study are newer (built after 1985) and larger ships (>10 000 GT), and acoustic measurements for these ships cover a wider frequency band (20–1000 Hz).

Because of these prominent differences, we only make general comparisons with previous studies.

In Fig. 5, the relationship between ship speed and source level is not obvious, unlike previous studies. For WWII merchant ships, Ross (1976) reported a positive relationship between overall source spectral level above 100 Hz and the size and speed of a vessel. The author, however, expressed caution in the use of this estimation formula for ships over 30 kGT, as is the case for most ships in this study. For container ships and vehicle carriers there is some evidence for an increase in radiated noise with an increase in speed. Figure 5 suggests that different functional relationships are needed for each ship-type, or at least class of ship. Given that ship-type is defined based on cargo carried, the design and operation of each ship-type will differ, resulting in differences in underwater radiated noise.

Results of this study provide important recommendations for building new models of shipping noise. First, it is inappropriate to combine multiple ship-types to derive functional relationships. There are fundamental differences in ship design characteristics that influence how the ships move
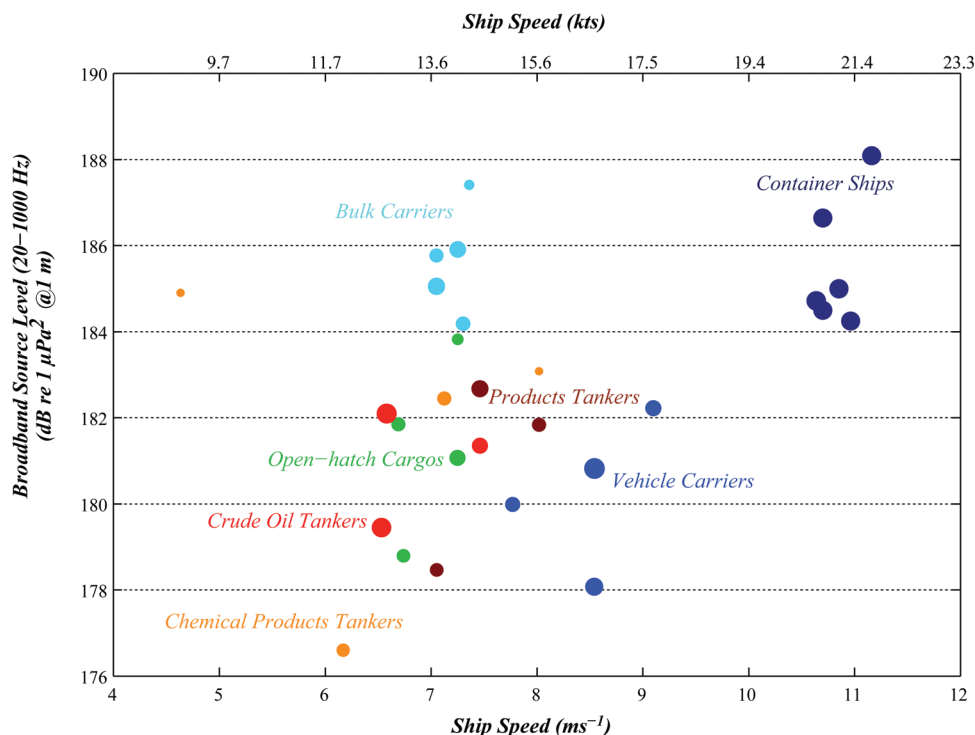
FIG. 5. Broadband ship source level versus speed for measured ships. Bubble color signifies ship-type. Bubble size represents the relative size of the ship, measured as GT from Table I.

through the water and likely result in differences in radiated noise, as seen in Fig. 5. We recommend that future studies predicting radiated ship noise should separate analyses by ship-type. Second, developing functional relationships with one or two variables (i.e., size and speed) will lead to inaccuracies in estimates of ship noise. With the advent of more advanced statistical methods, it is possible to more precisely predict shipping noise by including not only ship design and operating parameters, but also oceanographic conditions. Future studies with more ships in each ship-type category will provide new models of shipping noise for modern ships.

B. Unique ship acoustic signatures

Differences in the dominant frequency of radiated noise were found to be related to ship-type (Fig. 3). Bulk carrier noise is predominantly near 100 Hz while container ship and tanker noise is predominantly below 40 Hz. The tanker had less acoustic energy in frequencies above 300 Hz, unlike the container and bulk carrier. The causes of the distinct spectral characteristics are unknown but are relevant to ambient noise models and acoustic impact studies, and, therefore, should be a topic for future study.

It is possible these differences specific to each ship-type relate to operational differences, load of the ship, propeller type, or hull design. Fouling or damage on the propeller is unlikely to account for the major difference between ship-types because the same unique characteristics were observed in all ships of a given type (Fig. 4). On the other hand, Tanker 355799000 exhibits quite anomalously high SL given its speed, and this could be attributed to fouling or damage; however, it is also the oldest, shortest, and lowest HP ship listed in Table I.

Specific features of ship-types (e.g., source depth) might provide insight into the reason for similar estimated source levels for the bulk carrier and the container ships. A shallower source depth will decrease the effect of the dipole, thereby decreasing the amount of radiated sound from the ship in the horizontal direction. The closer the distance between the dipole sources, the less the strength of the dipole (Ross, 1976), as presented in this study's propagation models, when the source was moved from a depth of 14 to 7 m [Fig. 3(b)]. An unloaded ship likely results in a shallower depth of the propeller, thereby radiating less noise. Unfortunately, AIS does not provide information on the load of a particular ship during its transit; therefore, it is not possible to fully evaluate differences in radiated noise related to the ship load. However, the holds in bulk carriers must be full at all times to maintain the immersion of the propeller and prevent structural damage as required by a 2004 law passed by the Maritime Safety Committee of the International Maritime Organization (IMO) (Eyres, 2007). Container ships, on the other hand, do not always carry a full load, particularly ships traveling on a northbound route, as those measured in this study. A comparison of the spectral features of the same ship with varying cargo loads would help evaluate possible differences in radiated noise related to load.

Hull design is specific to each ship-type (Gillmer and Johnson, 1982; Eyres, 2007) and might also result in a difference in source depth between ship-types. Hull fullness, shape, and dimensions are optimized for efficient transfer of the goods carried. Hull design must balance the minimization of drag with structural integrity, stability, and practicality for transfer of goods at ports (Gillmer and Johnson, 1982; Ellefsen, 2010). Bulk carriers are full-form ships and have a

lower volumetric coefficient (i.e., ship displacement divided by the length between the perpendiculars cubed), compared to container ships (Gourlay and Klaka, 2007). In addition, hull design in container ships has been refined to promote efficient travel at faster speeds. Another feature of the container ships that might results in a shallower source depth is that they carry 60% of their cargo on deck, compared to all cargo below deck in bulk carriers (Eyres, 2007).

Vehicle carriers had the lowest source levels compared to the other ship-types in this study but were larger and traveled faster than the open hatch cargo ships and chemical tankers. Vehicle carriers have a high boxlike form that sits above the waterline to accommodate as many vehicles as possible on deck, resulting in a shallow draft and shallow propeller depths (Eyres, 2007), possibly explaining the lower measured source levels.

C. Predicting ship noise in the marine environment

This study provides data useful for marine noise models. Noise from commercial ship traffic is a dominant component of the low frequency noise in the deep-ocean; in coastal regions, the contribution of ship noise may also dominate the low frequency but is more difficult to predict (McDonald *et al.,* 2008; Hildebrand, 2009). The variability in ship noise in coastal regions relates to the proximity to shipping lanes and local sound propagation conditions, unlike deep water sites where distant shipping dominates ambient noise levels (Wagstaff, 1981; Bannister, 1986; Andrew *et al.,* 2002; McDonald *et al.,* 2006).

In building marine noise models, ship source levels are an important variable. The broadband ship source levels reported in this study are much higher than used in current worldwide shipping noise models such as ANDES (Carey and Evans, 2011). Incorporating the source levels of modern ships measured in this study will likely improve these models.

Quantifying ship traffic composition within a particular region will also improve marine noise predictions. Average noise levels and peak frequency bands will differ depending on the ship-types transiting the region. Bulk carriers have higher source levels near 100 Hz, compared to the much larger and faster container ships. This suggests that shipping models need to treat container ships independently from bulk carriers if they are to consider the entire spectrum below 200 Hz, where shipping noise dominates.

An asymmetrical pattern was observed in radiated noise for all ship-types, with stern aspect noise levels 5 to 10 dB higher than bow aspect noise levels. This was anticipated given that previous studies showed that source levels were generally higher at stern aspects compared to the bow (Arveson and Vendittis, 2000; Trevorrow *et al.,* 2008). The asymmetry may not matter for deep ocean shipping routes but could be significant when designing shipping channels near a marine protected areas or sensitive habitats.

D. Metrics for assessing noise impact

In this study, radiated ship noise over 1-h passages provided an estimate of both the spatial extent at which ship noise is elevated above background levels (Fig. 2) and the region within which potential impact of ship noise on marine organisms can be evaluated. Acoustic pollution from ship noise is considered one of the major factors affecting habitat quality for marine organisms (NRC, 2005). Concerns regarding acoustic noise pollution from ships arise because of the potential to disrupt natural habitat or cause injury to marine animals. Increased noise levels from ship traffic will interfere with marine organisms' ability to communicate and interpret acoustic cues in their environment; this is particularly relevant to baleen whales which call at frequencies similar to ship noise for mating-related behavior, long range communication, and coordination during foraging (Payne and McVay, 1971; Richardson *et al.,* 1995; Oleson *et al.,* 2007; Clark *et al.,* 2009). Acoustic masking compromises the receiver's ability to detect important acoustic signals in the same frequency range as the noise. By raising the background noise levels, ships will decrease the ranges at which animals can perceive calls from con-specifics (Clark *et al.,* 2009).

The SEL equations presented in this study provide a tool to estimate sound exposure levels of a passing ship. Sound exposure level represents the cumulative exposure to ship noise, important for understand potential acoustic impact. One assumption of the SEL calculation is that the source is moving away at a given speed and the receiver remains stationary over the integration time. For marine animals that have limited mobility, or in some cases highly mobile animals engaged in a site specific behavior, this is an accurate estimate of SEL. For organisms that are moving through this sound field, the SEL equations for each ship also allows SEL to be estimated if an animal moves towards or away from a ship during its passage.

E. Study limitations

The estimates of source levels presented in this study relied on accurate descriptions of the environment in which the sounds were generated. Some variability was expected related to differences in water column properties during each ship passage (Jensen *et al.,* 1993). To minimize error in the measurements, all ships were measured during the same time of year and using the same instrumentation. The use of AIS provided precise positions of the ship, which were interpolated and used to determine the distance of each ship to the HARP. The differences in CPA distances were small, resulting in minimal fluctuations in transmission loss (<3 dB).

A few limitations of the descriptions of ship noise presented are related to the opportunistic approach. Measurements were only made at broadside angles to the ship at distances of 3 km. This restricts descriptions of the directionality of radiated noise from individual ships. Previous studies with control over the movement of the ship relative to the acoustic receivers indicated that the radiation pattern was generally dipole in form. Some departures in this pattern in frequencies above 300 Hz suggest interactions with the hull, specifically, a decrease in the fore and aft directions by 3–5 dB (Arveson and Vendittis, 1996). This pattern has been widely observed and explained by others: bow radiation is blocked by the hull and stern radiation is partially absorbed

in the bubble wake of the ship (Matvee, 2005). Trevorrow *et al.* (2008) quantified this difference for a small coastal oceanographic vessel (560 GT). They reported a broadside maximum in source level, with a 12 dB reduction in the bow and a 9 dB reduction at stern aspect for large angles ($>40°$). These studies suggest that the estimates of the spatial extent of ship noise from broadside measurements in this study may be an overestimate for directly forward and aft of the ship.

The ship acoustic measurements were made near the seafloor and received levels are not necessarily representative of the levels throughout the entire water column. At these ranges and low frequencies, acoustic interference affects the radiated noise at a given range and depth. Both the depth of the sources and water column properties will influence this radiation pattern, as seen in the propagation models (Fig. 3). Autonomous hydrophone arrays with simultaneous water column sound speed profiles would improve these methods and provide a more comprehensive picture of radiated ship noise, using this same opportunistic approach.

Although this study only measured ship noise during a 1 month period to avoid variability related to seasonal differences propagation, the study is a sub-set of a larger database of noise measurements of ship passages. Future studies, with multiple examples of the same ship-type, will build on the methods presented in this study by deriving statistical relationships of underwater radiated noise from ship characteristics, operating parameters and oceanographic conditions.

Andrew, R., Howe, B., Mercer, J., and Dziecuich, M. (**2002**). "Ocean ambient sound: Comparing the 1960's with the 1990's for a receiver off the California coast," Acoust. Res. Lett. Online **3**, 65–70.

Arveson, P. T., and Vendittis, D. J. (**2000**). "Radiated noise characteristics of a modern cargo ship," J. Acoust. Soc. Am. **107**, 118–129.

Bannister, R. W. (**1986**). "Deep sound channel noise from high latitude winds," J. Acoust. Soc. Am. **79**, 41–48.

Bahtiarian, M. A. (**2009**). "ASA standard goes underwater," Acoust. Today, **5**(4), 26–29.

Carey, W. B., and Evans, R. B. (**2011**). *Ocean Ambient Noise, Measurement and Theory* (Springer, New York), p. 263.

Clark, C. W., Ellison, W. T., Southall, B. L., Hatch, L., Van Parijs, S. M., Frankel, A., and Ponirakis, D. (**2009**). "Acoustic masking in marine ecosystems: Intuitions, analysis, and implication," Mar. Ecol. Prog. Ser. **395**, 201–222.

Duncan, A. J., and Maggi, A. L. (**2005**). "Underwater acoustic propagation modeling software- AcTUP v2.2L," Centre for Marine Science and Technology, Curtin University, Australia.

Ellefsen, A. (**2010**). "The conceptual hull design," Det Norske Veritas http://www.dnv.com/industry/maritime/publicationsanddownloads/publications/dnvcontainershipupdate/2010/1-2010/theconceptualhulldesign.asp (Last viewed December 15, 2010).

Emery, K. O. (**1960**). "Basin plains and aprons off southern California," J. Geol. **68**, 564–479.

Eyres, D. J. (**2007**). *Ship Construction*, 6th ed. (Butterworth-Heinemann, Burlington, MA), p. 365.

Fisher, F. H., and Simmons, V. P. (**1977**). "Sound absorption in sea water," J. Acoust. Soc. Am. **62**, 558–564.

Gillmer, T. C., and Johnson, B. (**1982**). *Introduction to Naval Architecture* (U.S. Naval Institute, Annapolis, MD), p. 324.

Gourlay, T., and Klaka, K. (**2007**). "Full-scale measurements of containership sinkage, trim and roll," Aust. Nav. Arch. **11**(2), 30–36.

Hampton, L. (Ed.). (**1973**). *Physics of Sound in Marine Sediments* (Plenum Press, New York), p. 567.

Hatch, L., Clark, C., Merrick, R., Van Parijs, S., Ponirakis, D., Schwehr, K., Thompson, M., and Wiley, D. (**2008**). "Characterizing the relative contributions of large vessels to total ocean noise fields: A case study using the Gerry E. Studds Stellwagen Bank National Marine Sanctuary," Environ. Manage. **42**, 735–752.

Heitmeyer, R. M., Wales, S. C., and Pflug, L. A. (**2003**). "Shipping noise predictions: Capabilities and limitations," Mar. Technol. Soc. J. **37**.

Hildebrand, J. A. (**2009**). "Anthropogenic and natural sources of ambient noise in the ocean," Mar. Ecol. Prog. Ser. **395**, 5–20.

Hodgkiss, W. S., and Fisher, F. H. (**1990**). "Vertical directionality of ambient noise at 32°N as a function of longitude and wind speed," IEEE J. Oceanogr. Eng. **15**, 335–339.

Hulsemann, J., and Emery, K. O. (**1961**). "Stratification in recent sediments of Santa Barbara Basin as controlled by organisms and water character," J. Geol. **69**, 279–290.

Institute for Computational Earth System Sciences (ICESS) (2009). "Project and data description," http://www.icess.ucsb.edu/iog/realtime/index.php (Last viewed November 15, 2010).

Jensen, F. B., Kuperman, W. A., Porter, M. B., and Schmidt, H. (**1993**). *Computational Ocean Acoustics* (Springer, New York), p. 578.

Linder, C. A., and Gawarkiewicz, G. G. (**2006**). "Oceanographic and sound speed fields of the ESME workbench," IEEE J. Oceanogr. Eng. **31**(1), 22–32.

Mackenzie, K. V. (**1981**). "Nine-term equation for sound speed in the oceans," J. Acoust. Soc. Am. **70**, 807–812.

Matveev, K. I. (**2005**). "Effect of drag-reducing air lubrication on underwater noise radiation from ship hulls," J. Vib. Acoust. **127**, 420–422.

McClatchie, S., Goericke, R., Schwing, F. B., Bograd, S. J., Peterson, W. T., Emmett, R., Charter, R., Watson, W., Lo, N., Hill, K., Collins, C., Kahru, M., Mitchell, B. G., Koslow, J. A., Gomez-Valdes, J., Lavaniegos, B. E., Gaxiola-Castro, G., Gottschalck, J., L'Heureux, M., Xue, Y., Manzano-Sarabia, M., Bjorkstedt, E., Ralston, S., Field, J., Rogers-Bennet, L., Munger, L., Campbell, G., Merkens, K., Camacho, D., Havron, A., Douglas, A., and Hildebrand, J., (**2009**). "The state of the California current, spring 2008–2009. Cold conditions drive regional difference in coastal production," Progress Report No. 50, California Cooperative Oceanic Fishes Investigations, pp. 43–68.

McDonald, M. A., Hildebrand, J. A., and Wiggins, S. M. (**2006**). "Increases in deep-ocean ambient noise in the Northeast Pacific west of San Nicholas Island, California," J. Acoust. Soc. Am. **120**, 711–718.

McDonald, M. A., Hildebrand, J. A., Wiggins, S. M., and Ross, D. (**2008**). "A 50 year comparison of ambient ocean noise near San Clemente Island: A bathymetrically complex coastal region off Southern California," J. Acoust. Soc. Am. **124**, 1985–1992.

McKenna, M. F., Soldevilla, M., Oleson, E. M., Wiggins, S. M., and Hildebrand, J. A. (**2009**). "Increased underwater noise levels in the Santa Barbara Channel from commercial ship traffic and its potential impact on Blue Whales (*Balaenoptera musculus*)," in *Proceedings of the Seventh California Islands Symposium*, edited by C. C. Damiani, and D. K. Garcelon (Institute for Wildlife Studies, Arcata, California), pp 141–149.

National Research Council (NRC) (**2003**). *Ocean Noise and Marine Mammals* (National Academic Press, Washington, D.C.), pp. 83–108.

National Research Council (NRC) (**2005**). *Marine Mammal Populations and Ocean Noise; Determining When Noise Causes Biologically Significant Effects* (National Academic Press Washington, D.C.), pp. 23–34.

Oleson, E. M., Calambokidis, J., Burgess, W. C., McDonald, M. A., LeDuc, C. A., and Hildebrand, J. A. (**2007**). "Behavioral context of call production by eastern North Pacific blue whales," Mar. Ecol. Prog. Ser. **330**, 269–284.

Payne, R. S., and McVay, S. (**1971**). "Songs of Humpback Whales," Science **173**, 585–597.

Richardson, J. W., Greene, C. R. J., Malme, C. I., and Thomson, D. H. (Eds). (**1995**). *Marine Mammals and Noise* (Academic Press, San Diego, CA), pp. 576.

Ross, D. (**1976**). *Mechanics of Underwater Noise* (Pergamon, New York), pp. 272–287.

Ross, D. (**1993**). "On ocean underwater ambient noise," Inst. Acoust. Bull. **18**, 5–8.

Tetreault, B. J. (**2005**). "Use of the Automatic Identification (AIS) for maritime domain awareness (MDA)," in Proceedings of OCEANS 2005 MTS/ IEEE 2, 1590–1594.

Trevorrow, M. V., Vasiliev, B., and Vagle, S. (**2008**). "Directionality and maneuvering effects on a surface ship underwater acoustic signature," J. Acoust. Soc. Am. **124**(2), 767–778.

United Nations Conference on Trade and Development (UNCTD) (2008). "Review of maritime transport," http://www.unctad/org/en/docs/ rmt2008_en.pdf (Last viewed December 15, 2011).

United Nations Conference on Trade and Development (UNCTD) (2010). "Review of maritime transport," http://www.unctad/org/en/docs/ rmt2010_en.pdf (Last viewed March 5, 2010).

Wagstaff, R. A. (**1981**). "Low-frequency ambient noise in the deep sound channel—The missing component," J. Acoust. Soc. Am. **69**, 1009–1014.

Wales, S., and Heitmeyer, R. (**2002**). "An ensemble source spectra model for merchant ship-radiated noise," J. Acoust. Soc. Am. **111**, 1211–1231.

Wenz, G. M. (**1962**). "Acoustic ambient noise in the ocean: Spectra and sources," J. Acoust. Soc. Am. **34**, 1936–1956.

Wiggins, S. M., and Hildebrand, J. A. (**2007**). "High-frequency Acoustic Recording Package (HARP) for broad-band, long-term marine mammal monitoring," in *International Symposium on Underwater Technology 2007 and International Workshop on Scientific Use of Submarine Cables and Related Technologies* (Tokyo, Japan), pp. 551–557.

Wilmut, M. J., Chapman, N. R., Heard, G. J., Ebbeson, G. R. (**2007**). "Inversion of Lloyd Mirror Field for determining a source's track," IEEE J. Ocean. Eng. **32**, 940–947.